Rejuvenated stars are more easily unbound:
Stable mass transfer impacts the donor of common envelopes in gravitational wave progenitors

M. Renzo[1] AND

■ [others: R. Farmer, K. Breivik, E. Zapartas, Y. Gotberg, B. D. Metzger, M. Lau?] ■

[1]Center for Computational Astrophysics, Flatiron Institute, New York, NY 10010, USA

ABSTRACT

Common envelope (CE) evolution is an outstanding open problem in stellar evolution and it is critical to the formation of compact binaries, including gravitational-wave sources. In the "classical" isolated binary evolution scenario for double compact objects, the CE phase is usually the second mass transfer. Thus, the donor star of the CE is the product of a previous binary interaction, often a stable Roche lobe overflow (RLOF). Because of the accretion of mass, the convective core of the star grows and is "rejuvenated". This leads to a steeper core-envelope boundary which decreases significantly the envelope binding energy. Comparing accretor models from self-consistent binary models to stars evolved as single and models where we artificially impose specific core-envelope boundary profiles, we demonstrate that the "rejuvenation" caused by RLOF-accretion can significantly lower the amount of energy necessary for a CE ejection for both black hole and neutron star progenitors. ■ [quantitative statement about binding energy ratios] ■. Despite their high mass, our accretors also experience extended "blue loops" , which may have observational consequences for low-metallicity stellar populations and asteroseismology. Extending our small grid will be necessary to produce a rapid-population synthesis algorithm to account for this effect.

Keywords: stars: massive – stars: binaries: common envelope – stars: binaries: accretors

1. INTRODUCTION

Common envelope (CE) is an important evolutionary channel for massive isolated binaries to become gravitational-wave (GW) sources. Despite recent debates on its relevance for the progenitors of the most massive binary black holes (e.g., **?????**). CE remains a crucial step in the formation, among many other compact binaries, of cataclysmic variable (**?**), double white dwarfs (e.g., **???**), binary neutron stars (NS, e.g., **?**), merging black hole-neutron stars (e.g., **??**) and possibly low-mass binary black holes (BH, e.g., **??**).

In the "classical scenario" (e.g., **??**), a gravitational-wave progenitor system experiences a first mass transfer phase through Roche lobe overflow (RLOF) between two non-compact stars. Subsequently, the initially more massive donor collapses to a compact object without disrupting the binary (e.g., **??**). Only afterwards, as the initially less massive secondary expands, a second mass-transfer phase occurs and is typically dynamically unstable, that is a CE (e.g., **???**). This second mass transfer is responsible for the orbital shrinking (**?**) allowing the system to merge within the age of the Uni-

verse. Therefore, in this scenario, the donor star of the CE is the former accretor of the first RLOF (e.g., **???**).

The first stable RLOF typically occurs during the main sequence of the initially less massive star and accretion modifies its structure (e.g., **?????**). On top of the enrichment of the envelope with CNO-processed material from the donor star core (**???**), and the substantial spin-up, accretors are expected to adjust their core-size to the new mass in a "rejuvenation" process (e.g., **???**). The readjustment is driven by mixing at the boundary between the convective core and the envelope, which re-fuels the convective region of hydrogen. This mixing also affects the entropy, density, and binding energy profile of the core-envelope boundary (CEB) layer (**?**), where the density rises and most of the binding energy is accumulated. Consequently, the success or failure of the CE ejection, which is likely decided in the CEB layer (e.g., **?**), may be different depending on whether the CE-donor accreted mass previously or not.

Here, we use structure and evolution binary models to study the impact of the first RLOF phase on the outcome of possible subsequent CE events. Sec. **??** describe our `MESA` calculations, and Sec. **??** presents a proof-of-

principle of the effect of core boundary mixing and rotation on the envelope binding energy. In Sec. **??** we compare our accretor models to single stars with the same total post-RLOF mass. We discuss our findings and conclude in Sec. **??**.

2. PRE-COMMON ENVELOPE EVOLUTION

We use `MESA` (version 15140, **?????**) to compute the evolution of binaries which experience mass transfer after the end of the donor's main sequence, that is case B Roche lobe overflow (RLOF, **?**). Our setup[1] is similar to **?**, except for the metallicity: here we adopt $Z = 0.0019 \simeq Z_\odot/10$, relevant for the progenitor population of GW events (e.g., **?**). Moreover, we apply throughout the star a small amount of mixing with diffusivity `min_D_mix`=100. This improves the numerical stability by smoothing properties across adjacent cells, without introducing significant quantitative variations, and is a typical numerical trick used in asteroseismology calculations (J. Fuller, private comm.).

We adopt initial period $P = 100$ days and chose initial masses $(M_1, M_2) = (18, 15), (20, 17), (38, 30)\, M_\odot$. We focus on the initially less massive stars, which post-RLOF with our setup described below become $M_2 = 15 \to 18, 17 \to 20, 30 \to 36\, M_\odot$, roughly[2] representative of NS, uncertain core-collapse outcome, and BH progenitors, respectively. Our `MESA` models assume that the accretion efficiency is limited by rotationally enhanced wind mass loss (e.g., **????**). However, this may lead to less conservative mass transfer than suggested by observations (e.g., **?**).

To avoid computing the late evolutionary phases of the donors, and focus on the post-RLOF evolution of the accretors, after detachment from the Roche lobe, our simulations artificially separate the stars and continue the evolution of the secondary as a single star until it reaches carbon depletion (defined by central carbon mass fraction $X_c(^{12}C) < 2\times10^{-4}$). We make the routine to detach a `MESA` binary on-the-fly publicly available[3]. This approach implies that we neglect further binary interactions (e.g., tides, case BB RLOF, **?**), the impact of the core-collapse of the RLOF-donor on the accretor (e.g., **??**) and on the orbit (e.g., **????**).

To illustrate the physical reason why the first RLOF may influence the envelope structure of the accretor much later on, we also compute comparison single stars

---

[1] Available at 10.5281/zenodo.6600641.

[2] Whether a core-collapse results in NS or BH formation, with or without an associated explosion, cannot be decided solely based on the (total or core) mass of a star (e.g., **?????**).

[3] https://github.com/MESAHub/mesa-contrib/

Figure 1. TAMS entropy profile of a single $30\, M_\odot$ star (red) and engineered models where we artificially modify the CEB region (gray shaded area). The CEB for a single $30\, M_\odot$ star has a mass of $5.81\, M_\odot$ at TAMS, while the engineered models span the range $\sim 3 - 9.4\, M_\odot$.

with the same setup, and "engineered" stars which we modify at terminal age main sequence (TAMS, central hydrogen mass fraction $X_c(^1H) < 10^{-4}$). Fig. **??** shows an example grid for $30 M_\odot$, with the gray area highlighting the region where models have been modified (corresponding to H mass fraction $X_c(^1H) + 0.05 < X(^1H) < X_{surf}(^1H) - 0.05$, with X_c and X_{surf} the central and surface value of the hydrogen mass fraction). More specifically, we modify the CEB specific entropy (s), hydrogen (H), and helium (He) profiles. Starting from a non-rotating single star at TAMS (e.g., red model in Fig. **??**), we maintain the same inner and outer profiles, but impose a linear connection from the outer boundary of the H-depleted core to a mass coordinate which we specify as a parameter (see Fig. **??** and Fig. **??**). We let `MESA` "relax" the TAMS profiles to the desired entropy and composition profiles, and then evolve until either carbon depletion or when these models first exceed $1000\, R_\odot$. These "engineered" stars with artificially imposed CEB structures mimic in an oversimplified way the impact of RLOF-driven rejuvenation of the accretors.

We compare the internal structure of accretors to single and engineered stars at various radii ($R = 100, 200, 300, 500, 1000\, R_\odot$). At the onset of a CE event, $R \equiv R_{RL,donor}$ is the size of the Roche lobe of the donor

star determined by the binary separation and mass ratio (e.g., **??**).

■ [**possibly move two next section as appendixes to try letter**] ■

3. IMPACT OF CORE-ENVELOPE BOUNDARY AND ROTATION ON THE BINDING ENERGY PROFILE

Before focusing on binary evolution models, we start by illustrating with examples how the envelope binding energy depends on the CEB layer (Sec. **??**) and on the initial rotation rate of the star (Sec. **??**). Both can be significantly modified by accretion during the first RLOF.

3.1. Steepness of the core-envelope boundary

Fig. **??** shows a comparison of the gravitational and binding energy profiles of a $30\,M_\odot$ single star (red solid line) to "engineered" models (see Sec. **??**), when stars first reach radius $R = 500\,R_\odot$. We define the gravita-

Figure 2. The structure of the CEB impacts the envelope gravitational binding energy profile throughout the remaining evolution. Dashed lines show the gravitational contribution only, while solid lines include the contribution of the internal energy. The red lines show a $30\,M_\odot$, non-rotating, $Z = 0.0019$ model compared to "engineered" models of the same mass, but artificially imposed profile at TAMS (other colors, see text). Models are compared when they first reach $500\,R_\odot$, while the inset panel shows the entropy profiles at TAMS (when we artificially modify the "engineered" stars).

tional binding energy as (e.g., **???**):

$$BE(m, \alpha_{\rm th}) = -\int_m^M dm' \left(-\frac{Gm'}{r(m')} + \alpha_{\rm th} u(m') \right) \quad (1)$$

with M total mass of the star, $r(m')$ radius, $u(m')$ the internal energy of a shell of mass thickness dm' and outer Lagrangian mass coordinate m', and G the gravitational constant. The integral domain goes from mass coordinate m, which can be thought of the mass of the "core" surviving a hypothetical CE, to the surface. The parameter $0 \leq \alpha_{\rm th} \leq 1$ is the fraction of internal energy (including recombination energy) that can be used to lift the shared CE. It is possible that $\alpha_{\rm th}$ may not be constant during a CE. For $\alpha_{\rm th} = 0$, Eq. **??** reduces to $BE(m, \alpha_{\rm th} = 0) \equiv -E_{\rm grav}(m)$ (dashed lines in Fig. **??**), while $\alpha_{\rm th} = 1$ assumes perfectly fine tuned use of all the internal energy (solid lines). These two cases bracket the range of possibilities.

Fig. **??** shows that the gravitational and binding energy depend on the structure of the CEB region. In single stars, the CEB is determined by the extent of the convective boundary mixing and, more importantly, the recession in mass coordinate of the convective region. In Fig. **??**, lines of different colors show a trend with shallower entropy and composition profiles at TAMS (lighter curves in Fig. **??**) evolving into more gravitationally bound inner envelopes (larger binding energy inside $\log(r/\text{cm}) \lesssim 11$), and viceversa.

3.2. Rotation

Mass transfer through RLOF from a binary companion also spins up the accreting star, often to critical rotation[4] (e.g., **???**). Although spinning up a star late during its main-sequence evolution has a different structural consequences than natal rotation (see **?**), our accretor models can reach a rigid, close-to-critical rotation late during RLOF. Thus, it is worth considering the impact of rotation on the envelope structure and CEB by analyzing single star models rotating since birth.

Rotation has a two main effects: (i) mixing can change directly the core size (see **??**), (ii) changes in the mass-loss rate (e.g., **???**) affect the rate of recession of the convective core (e.g., **??**). By inflating the equatorial region, rotation changes the temperature and opacity structure, and therefore the line-driving of the wind. Moreover, rotation can have a dynamical effect, resulting in mass loss through the combination of centrifugal

---

[4] At critical rotation, the centrifugal force balances the gravitational pull at the equator, corresponding to angular frequency $\omega_{\rm crit} = \sqrt{(1 - L/L_{\rm Edd})GM/R^3}$ is the critical spin frequency, with $L_{\rm Edd}$ the Eddington luminosity, and L is the luminosity.

Figure 3. Same as Fig. **??** but comparing single stars differing by their initial rotation rate.

forces and radiative pressure ($\Gamma - \Omega$ limit, **?**). Onedimensional stellar evolution codes commonly assume that rotation increases the total mass loss rate (e.g., **??**) though this may not be true throughout the evolution (e.g., **?**).

Fig. **??** shows the gravitational binding energy profile of the single $30\,M_\odot$ star of Fig. **??**, compared to single stars of the same mass and varying initial $\omega/\omega_{\rm crit}$. For $\omega/\omega_{\rm crit} \lesssim 0.5$, corresponding to a generous upper-bound for the typical birth rotation rate of single massive stars (e.g., **?**), the effect is modest but non-negligible. For more extreme initial rotation rates (achievable during RLOF, at least in the surface layers), the ratio of the He core mass to total mass is significantly changed by rotational mixing, which can result in larger binding energy differences than changing the CEB layer at fixed core mass.

In accretors in binary systems both the effect illustrated in Fig. **??** and Fig. **??** act simultaneously, although the timing and amplitude of the impact of mixing and rotation can be different than for single stars (**?**).

4. ACCRETORS FROM SELF-CONSISTENT BINARY MODELS

We now consider accretors computed self-consistently in a binary until detachment, and subsequently as single stars until carbon core depletion. Fig. **??** shows the evolution of our binaries on the Hertzsprung-Russell (HR)

diagram. The thin dashed lines show the evolution of the donor stars from TAMS, through RLOF, until our definition of detachment (see, e.g., **?????**). The solid lines correspond to the full evolution of the accretors, from zero age main sequence (ZAMS), through RLOF (see **???**), until carbon depletion.

Figure 4. HR diagram of the binary systems. The thin dashed lines show the evolution of the donors until RLOF detachment, the solid lines show the accretors from ZAMS, through RLOF accretion, until core carbon depletion. Thin dot-dashed lines mark constant radii of $R = 100, 200, 300, 500, 1000\,R_\odot$, all models have $Z = 0.0019$, period $100\,{\rm days}$, and initial masses of 38 and $30\,M_\odot$ (green), 20 and $17\,M_\odot$ (orange), 18 and $15\,M_\odot$ (blue). ■ [**annotate key epochs?**] ■

■ [**how long the blue loops**] ■ All three accretor models experience a blue-loop after beginning to ascend the Hayashi track. Blue loops are not expected for single stars with $M \gtrsim 12\,M_\odot$ (e.g., **?**), and their occurrence is known to be sensitive to the He profile above the H-burning shell, and specifically the mean molecular weight profile (**??**). Thus it is not surprising that RLOF-accretion, which modifies the stellar profile above the H-shell, may lead to blue loops, and formation of yellow-supergiants (e.g., **?**). We note that comparison single stars also experience a late blue-ward evolution, but not a "loop" back to red. This behavior is likely related to the relatively high wind mass-loss rate assumed (see **?**), and the models with initial mass $\gtrsim 30\,M_\odot$ are qualitatively similar to the most massive accretor in

Fig. **??** even without accreting matter from a companion: the occurrence of blue loops is notoriously sensitive to many single star physics uncertainties, and while the appear consistently in our accretor models their physicality should be tested further.

However, in the context of GW progenitors, blue loops are not crucial since they correspond to a decrease in radius, which would not result in binary interactions during the loop. They might change the mass-loss history of the accretor, but since they occur in a short evolutionary phase, their impact should be limited.

Fig. **??** shows the entropy, H and He mass fraction profiles at TAMS for our accretor models (orange), single non-rotating stars (red) and "engineered" models of the same mass as the accretor post-RLOF. We chose to compare our accretors to models of the same total mass, since this quantity appears in the envelope binding energy (see Eq. **??** and e.g., **??**). Nevertheless, it is not obvious that this is the most relevant comparison: for instance, the (He or carbon-oxygen) core mass is often used to determine the final compact object (e.g., **?????**), and comparing models of roughly the same coremass might be more appropriate (but is sensitive to the condition defining the core edge). We present in Fig. **??** a comparison between TAMS profiles of accretors, single stars, and engineered models with the same *initial* mass as an alternative comparison that should bracket the range of sensible comparison models.

Accretion through RLOF affects the CEB layer in more subtle ways than we impose in our "engineered" models. One expects the CEB in accretors to be steeper than in a star evolving as single, resulting in models qualitatively more similar to our engineered models with the steeper CEB (darker lines in Fig. **??**-**??**, Fig. **??**-**??**, and Fig. **??**-**??**). In fact, rejuvenation of the accretor is caused by an increase in mass coordinate of the convective core (and consequent refueling of H in the core): this is a thermal process related to convection and convective boundary mixing. Since the convective turnover timescale in the core of a massive star is shorter than (i) the nuclear timescale – over which the composition of the core changes, (ii) the donor thermal timescale – governing case B RLOF mass-transfer, and (iii) the accretor thermal timescale – governing the thermal readjustment of the star, the increase in mass coordinate of the core should create a steep composition and entropy gradient at the new (post-accretion) outer edge. In practice, binary interactions occur after a finite amount of the accretor's main-sequence has elapsed. This pre-RLOF duration depends on the period and mass ratio of the two stars. For our binaries with initial $P = 100\,\mathrm{days}$ and $q = M_2/M_1 \simeq 0.8$, RLOF starts after $\sim 10, 9,$

and $5\,\mathrm{Myrs}$ from the least massive to the most massive binary, which correspond to central H mass fractions $X_\mathrm{c}(^1\mathrm{H}) = 0.27, 0.23,$ and 0.21 for the accretors. Thus, the accreting stars are not homogeneous in composition at the onset of RLOF: the convective core is already bound by a composition gradient that generally impedes the mixing (e.g., **?**). Thus, the advance in mass coordinate of the convective region due to mass accretion (i.e., the "rejuvenation process") during RLOF occurs against a gradient (of entropy, μ, H, and He) set by the pre-RLOF evolution.

To quantify the impact of the first RLOF phase on the outcome of the second mass transfer phase, we evolve in time all the TAMS profiles shown in Fig. **??** and compare them at fixed outer radii. In Fig. **??**, we show the binding energy (solid lines, including the internal energy, i.e. $\alpha_\mathrm{th} = 1$) of our accretor models, single stars with initial mass roughly equal to the accretors post-RLOF mass, and our engineered models (see also Fig. **??** for the λ_CE profile) The two lowest mass accretors (left and central column) do not expand to $R = 1000\,R_\odot$ before carbon depletion. Generally speaking, the accretors (orange) have lower binding energies than corresponding single stars (red), and their profiles are qualitatively closer to the engineered models with the steepest core (dark green curves), although local deviations from this trend can occur for some r.

4.1. *Ratio of binding energies as a function of mass*

Because of the large range of BE across the stellar structures, it is hard to appreciate the magnitude of the effect of RLOF-driven rejuvenation on the structure of the stars in Fig. **??**. Figure **??** presents the ratio of the local binding energies of our accretor models divided the local binding energy of comparison single stars, as a function of radius. To compute the ratio, we interpolate linearly the single star models on the mesh of our accretor, using the fractional Lagrangian mass coordinate m/M as independent coordinate. We calculate these ratio when both the stars reach for the first time radii $R = 100, 200, 300, 500, 1000\,R_\odot$ (see vertical gray dashed lines), corresponding to the assumed Roche lobe radius of the donor at the onset of the CE.

In each panel, radial coordinates r for which the lines in Fig. **??** are below one correspond to radii at which the accretor models are less bound than the comparison single star or engineered model. In other words, it would take less energy to eject the outer layers of the envelope of the accretors down to such r. All of our accretor models, regardless of them being NS or BH progenitor, and regardless of their evolutionary phase, produce envelope structures ($r \gtrsim 10^{10}$ cm) that are less bound than

Figure 5. Specific entropy (top row), H (bottom row, solid lines), and He (bottom row, dashed lines) TAMS profiles for non-rotating single stars (red), accretors (orange), and "engineered" models of the same total mass as the post-RLOF mass of the accretors. The gray bands emphasize the CEB region, which is well defined at TAMS.

the corresponding non-rotating single star models (red), and which are qualitatively more similar to the darker lines representing engineered models with steeper CEB profiles.
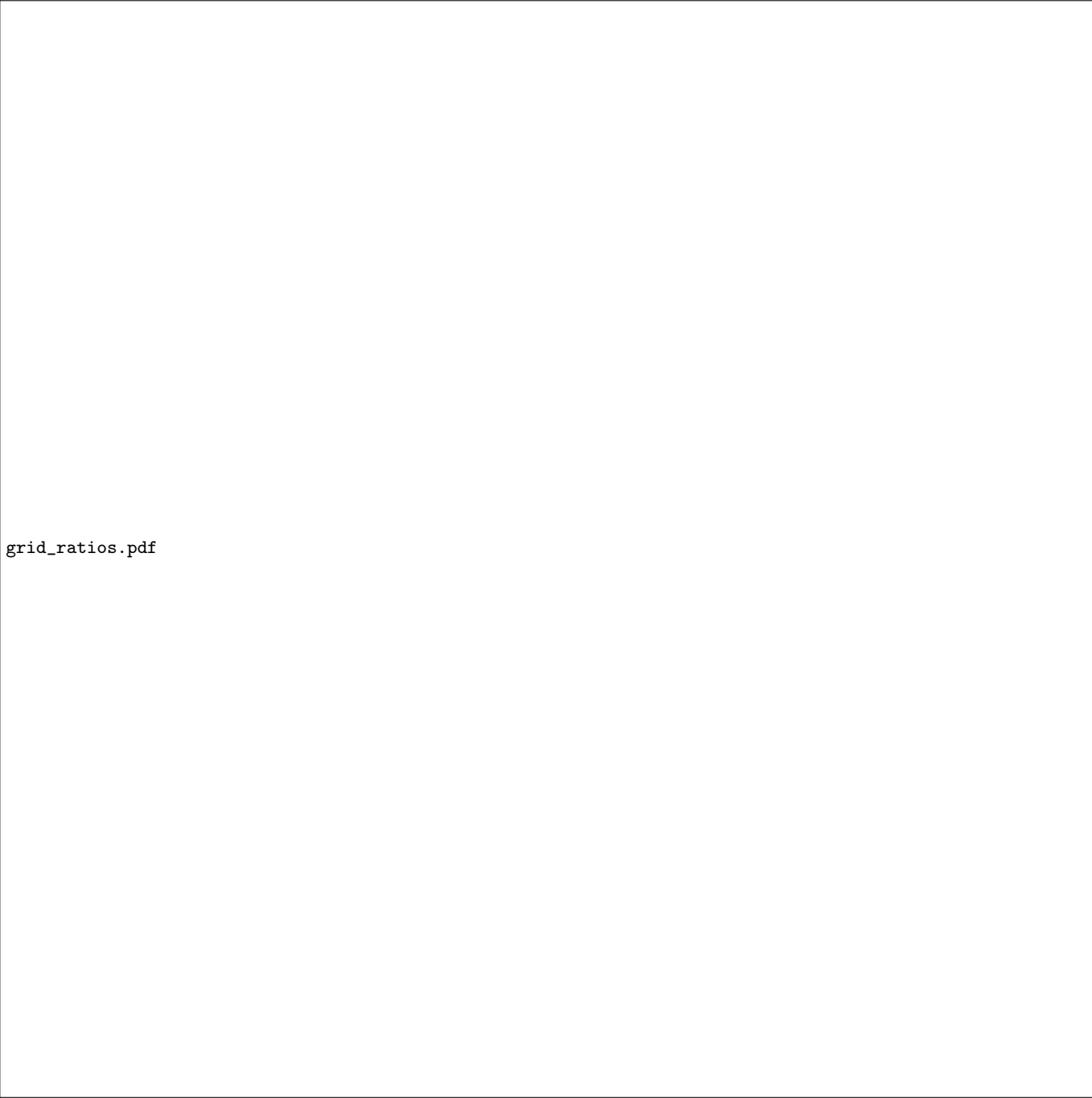
The minimum ratio of binding energies occur roughly at the inner edge of the the CEB layer in Fig. **??**. Considering the ratio to single stars (red lines), the minima range between 0.56-0.07; 0.58-0.08; and 0.51-0.04 from

our least to most massive binary. In other words, at the radius where the difference between accretors and single stars models is largest, which is also the location where the outcome of a common envelope is likely to be decided (e.g., **?**), the accretor's binding energy is roughly between $\sim 50 - \mathrm{few}\%$ of the binding energy of a single star. Regardless of the mass, the larger the outer radius the smaller the minimum of the ratio of binding

Figure 6. Binding energy profile at fixed radii (right y-axis) as a function of radial mass coordinate. We only show profiles with $\alpha_{\mathrm{th}} = 1$, that is accounting for the internal energy content of the star. Orange, red, and other colors show respectively the accretor models, single stars of same post-RLOF total mass, and engineered models with varying CEB steepness. Titles indicates the pre-RLOF and approximate post-RLOF accretor masses, and vertical gray dashed lines mark the total radius R of these models.

grid_ratios.pdf

Figure 7. Ratios of the binding energy profiles (including internal energy) of the accretor stars divided stars of the same total mass post-RLOF. The red solid lines show the ratio to a non-rotating single star, while the other colors show the ratio to "engineered" star (see text). Each panel shows the ratios at the first time the models reach the radius indicated on the right and by the vertical dashed gray line.

energies: the differences caused by RLOF accretion and rejuvenation of the core grows the stars evolve and their core contract.

Defining the He core boundary as the outermost location where $X < 0.01$ and $Y > 0.1$, we can fix $m = M_{\mathrm{He}}$ in Eq. **??** to obtain an integrated binding energy for the envelope:

$$BE_{\mathrm{env}} \equiv BE(m = M_{\mathrm{He}}, \alpha_{th} = 1) \ \ . \qquad (2)$$

Fig. **??** shows the evolution of this integrated envelope binding energy as a function of the outer radius. Each panel shows one of our binaries, from top to bottom: $36+30\,M_\odot$, $20+17\,M_\odot$, $18+15\,M_\odot$. The dashed lines correspond to single stars with the same total mass as the accretors post-RLOF, while solid lines correspond to the accretors. For each binary, the lower panel shows the ratios of the envelope binding energy of the accretor divided the binding energy of the comparison single star (i.e., the ratio of the solid lines to the dashed lines in the panel above). To compute these ratios, we interpolate our accretor models on the time-grid of the single stars using the central temperature $\log_{10}(T_c/[\mathrm{K}])$ as independent coordinate. In each of the lower panels the ratios are lower than one (marked by the gray dashed lines) at almost all radii, again suggesting that post-RLOF, accretor stars have envelopes that require less energy input to be ejected in a CE event.

BE_env_R.pdf

Figure 8. Evolution as a function of the photospheric radius R of the binding energy (including the thermal energy, $\alpha_{\mathrm{th}} = 1$) of the accretors and single stars of the same (post-RLOF) total mass. The bottom panels show the ratio, which is always smaller than 1, indicating that the accretors might have envelopes easier to unbind in a common envelope event.